Rapid Communications

Fourier heat conduction as a strong kinetic effect in one-dimensional hard-core gases

Hanqing Zhao[1,2] and Wen-ge Wang[1]

[1]*Department of Modern Physics, University of Science and Technology of China, Hefei 230026, China*

[2]*School of Physical Science and Technology, Key Laboratory for Magnetism and Magnetic Materials of MOE, Lanzhou University, Lanzhou, Gansu 730000, China*

(Received 6 October 2017; published 19 January 2018)

For a one-dimensional (1D) momentum conserving system, intensive studies have shown that generally its heat current autocorrelation function (HCAF) tends to decay in a power-law manner and results in the breakdown of the Fourier heat conduction law in the thermodynamic limit. This has been recognized to be a dominant hydrodynamic effect. Here we show that, instead, the kinetic effect can be dominant in some cases and leads to the Fourier law for finite-size systems. Usually the HCAF undergoes a fast decaying kinetic stage followed by a long slowly decaying hydrodynamic tail. In a finite range of the system size, we find that whether the system follows the Fourier law depends on whether the kinetic stage dominates. Our Rapid Communication is illustrated by the 1D hard-core gas models with which the HCAF is derived analytically and verified numerically by molecular dynamics simulations.

DOI: 10.1103/PhysRevE.97.010103

Driven by applications of nanomaterials, heat conduction properties of low-dimensional materials have been a focus topic in the past three decades [1–8]. Based on numerous theoretical studies, it is concluded that, in general, the thermal conductivity of a low-dimensional momentum conserving system has a system-size-dependent abnormality in the thermodynamic limit [9–11]. This abnormality is attributed to the hydrodynamic effect that induces the slow power-law decay of the heat current autocorrelation function (HCAF) [9,10]. However, real materials have a finite system size, hence whether this abnormality applies to a finite system needs to be carefully examined. Indeed, counterexamples, i.e., momentum conserving systems but yet having a size-independent thermal conductivity, have been found in simulations of finite systems [11–14]. These counterexamples usually have asymmetric interparticle interactions, including the Toda-like models [13], the Lennard-Jones model [11,12,14], the Fermi-Pasta-Ulam-α-β model [11], the diatomic gas model [15,16], the diatomic Toda model [16], and so on. More importantly, so far the direct experimental measurement results of the thermal conductivity of low-dimensional materials are also divergent. For example, for graphene, some studies confirm that its heat conduction behavior is abnormal [17] but others support that it is normal [18].

In the one-dimensional (1D) case, the heat conductivity, denoted by κ, is related to the HCAF, denoted by $C(t)$, by the Green-Kubo formula,

$$\kappa = \lim_{t_c\to\infty}\lim_{L\to\infty}\frac{1}{k_B T^2 L}\int_0^{t_c} C(t)dt. \tag{1}$$

Here k_B is the Boltzmann constant, L and T are, respectively, the size and the temperature of the system, $C(t) \equiv \langle J(0)J(t)\rangle$ with $J(t)$ being the total heat current at time t, and $\langle\cdot\rangle$ representing the equilibrium ensemble average. For a finite system, Lepri *et al.* [3] suggest to drop the limits and truncate the integral at $t_c = L/c_s$ (c_s is the sound speed) to calculate the heat conductivity [3,11]. It leads to $\kappa \sim L^{1-\alpha}$ in the thermodynamical limit given that $C(t)$ tends to decay as $\sim t^{-\alpha}$ as $L \to \infty$.

In trying to understand the aforementioned counterexamples and the existing experimental results, Chen *et al.* conjectured that the asymmetric interactions may practically lead to a size-independent thermal conductivity in a certain finite system-size range [11] because the hydrodynamic approach may not apply to systems of asymmetric interactions in a transient but maybe long time period. In this transient period, the HCAF may decay faster, but its contribution to the thermal conductivity can dominate until that contributed by the hydrodynamic power-law tail becomes comparable after a sufficiently long time. Therefore, although the predicted abnormality can be the case in the thermodynamics limit, normal heat conduction following the Fourier law can still be expected in a finite system-size range. This would have significant practical implications because any real materials are in fact finite.

It is thus important to establish a complete theory based on which the kinetic effect can be evaluated and taken into account as well. This is our motivation, and in this Rapid Communication, we will focus on the 1D diatomic gas [19], a paradigmatic momentum conserving fluid model. The hard-core elastic collision occurring when two neighboring particles meet can be considered as an effective asymmetric interaction. It is worth noting that there has been a long-term argumentation towards the heat conduction property of this model. In 2001, Garrido *et al.* presented the numerical evidence to show that this model has a convergent thermal conductivity in the thermodynamic limit [20]. This result was questioned by many other authors [21–23] because of the clear power-law decaying tail in the HCAF. Nevertheless, a recent numerical study showed that, interestingly, when the two types of particles in the system have close masses, the heat conductivity does not depend on the system size in a certain system-size range [16]. Moreover, it

is observed that the HCAF shows an exponential-like decay in a transient stage and the time this transient stage lasts increases rapidly as the mass ratio tends to 1. Therefore, the mass ratio is a key parameter for the heat conduction property of this model. In view of the subtlety of this issue and the limitation of the numerical simulations, an analytical study is particularly desired. In the following we will show that the idea of the conventional kinetic approach can be borrowed for our aim here.

First of all, suppose that our model consists of N particles with alternative masses μ_1 and μ_2 queueing on a line. We assume that $\mu_1 > \mu_2$ and define $r = \mu_1/\mu_2$ as the mass ratio. Let m_i and v_i be the mass and velocity of the ith particle; after a collision, the velocities of the two neighboring particles, say the ith and the $(i+1)$-th, change into

$$\begin{aligned} v_i(t+1) &= \frac{m_i - m_{i+1}}{m_i + m_{i+1}} v_i(t) + \frac{2m_{i+1}}{m_i + m_{i+1}} v_{i+1}(t), \\ v_{i+1}(t+1) &= \frac{m_{i+1} - m_i}{m_i + m_{i+1}} v_{i+1}(t) + \frac{2m_i}{m_i + m_{i+1}} v_i(t), \end{aligned} \tag{2}$$

where the time t is measured as the number of collisions. Note that this dynamics keeps the total momentum and energy of the system.

In the kinetic theory, for characterizing the Brownian motion, one traces a tagged particle and studies the decay of its velocity autocorrelation function. In our model a particle is always bounded by its two neighbors. Hence, instead of tracing a tag particle, we record the energy the tagged particle carries initially, which we term as the "tagged energy," and investigate how it spreads over the system. Note that during a collision, the energy carried by a particle will separate into two parts; one part remains on itself, whereas another part transfers to the other particle. If the two particles have close masses, then the transferred part will hold a large proportion. For the sake of convenience, in the following we term this transferred part of energy as the dominant energy since it dominates the decay behavior of the HCAF before the hydrodynamic process takes over. Similarly, we term the particle that carries the dominant energy as the dominant carrier. (At a given time there is only one dominant carrier.) Then the tagged energy can be traced by following the ensuing dominant energy sequence and in turn by tracing the dominant carriers. This is the key technique we adopt for our analytical treatment, which can be seen as an extension of the conventional kinetic approach.

As an example, let us take the ith particle as the tagged particle and assume its first collision happens with the $(i+1)$-th particle. According to Eq. (2), after the collision its initial velocity $v_i(0)$ separates into two parts, the remaining part $\frac{m_i - m_{i+1}}{m_i + m_{i+1}} v_i(0)$ and the transferred part $\frac{2m_i}{m_i + m_{i+1}} v_i(0)$. For $m_1 \approx m_2$, the remaining part will be much smaller than the transferred part, and the $(i+1)$-th particle thus carries the dominant energy and becomes the dominant carrier. As the velocity component $\frac{2m_i}{m_i + m_{i+1}} v_i(0)$ in $v_{i+1}(1)$ comes from $v_i(0)$, it correlates with $v_i(0)$. Similarly, when the next collision happens between the $(i+1)$-th particle and one of its neighbors [no matter the ith particle or the $(i+2)$-th particle as they have the same masses], the transferred velocity that contains $v_i(0)$ is $\frac{4m_i m_{i+1}}{(m_i + m_{i+1})^2} v_i(0) = \frac{4r}{(1+r)^2} v_i(0)$. It is thus straightforward that, after $2P$ collisions, the portion of $v_i(0)$ that transfers to the dominant carrier is

$$v_i(0) \left[\frac{4m_i m_{i+1}}{(m_i + m_{i+1})^2} \right]^P = v_i(0) \left[\frac{4r}{(1+r)^2} \right]^P. \tag{3}$$

Now let us consider the HCAF. The total energy current is defined as $J(t) \equiv \sum_q^N j_q(t)$, where $j_q(t) \equiv \frac{1}{2} m_q v_q^3(t)$ is the local current on the qth particle. Still taking the ith particle as the tagged particle, we have [3,13]

$$\langle J(t) J(0) \rangle = N \sum_q^N \langle j_q(t) j_i(0) \rangle. \tag{4}$$

Suppose that at time $t = 2P$ the dominate carrier is the kth particle and t_F is the average time for the dominant energy transferring from one dominant carrier to the next; for $r \to 1$, we have $j_q(t) j_i(0) \neq 0$ for $q = k$, and the other $j_q(t) j_i(0)$ terms are negligible. This gives that

$$C(t) = N \left[\frac{64 r^3}{(r+1)^6} \right]^{t/(2t_F)} \langle j_i(0) j_k(0) \rangle, \tag{5}$$

which can be rewritten as

$$C(t) = C(0) e^{-(t/\tau)}, \tag{6}$$

with

$$\tau = -2t_F \left[\ln \left(\frac{64 r^3}{(r+1)^6} \right) \right]^{-1}. \tag{7}$$

Equations (6) and (7) are our main result, which indicate that the HCAF decays exponentially in the kinetic stage. The physics picture behind Eq. (6) is indeed similar to that of the Brownian motion. In our case, the tagged particle is bounded, but its energy is dispersed due to the interactions with and among the surrounding particles, resulting in an exponentially decaying energy current autocorrelation function. In our model, the dominant carrier changes from one to another. During this process, the tagged energy keeps losing so that the HCAF, dominated by the remaining energy of the dominant carrier, decays exponentially. Therefore, our treatment is the same in spirit as the conventional kinetic approach. The parameter to be determined is t_F. As is generally accepted that the energy is transported by the sound modes [24,25], it is reasonable to assume that the energy is transferred at the sound speed as well, and therefore we have $t_F = \frac{a}{c_s}$, where a is the average distance between two neighboring particles (throughout this Rapid Communication we set $a = 1$ so that $N = L$). Note that an improved estimation of t_F should take into consideration the local energy density.

By substituting (6) into the Green-Kubo formula (1), we can obtain the thermal conductivity due to the kinetic effect exclusively,

$$\kappa_k = \frac{\tau}{k_B T^2} C(0). \tag{8}$$

When the hydrodynamic contribution is negligible in a finite system, we have $\kappa \approx \kappa_k$. In fact, as the dominant energy keeps losing [see Eq. (3)], the energy transferred to other particles cannot be neglected after a sufficiently long time. This part of the energy evolves following the hydrodynamics and can be captured by the hydrodynamics approaches [10]. The decaying behavior of the HCAF induced by the hydrodynamics process

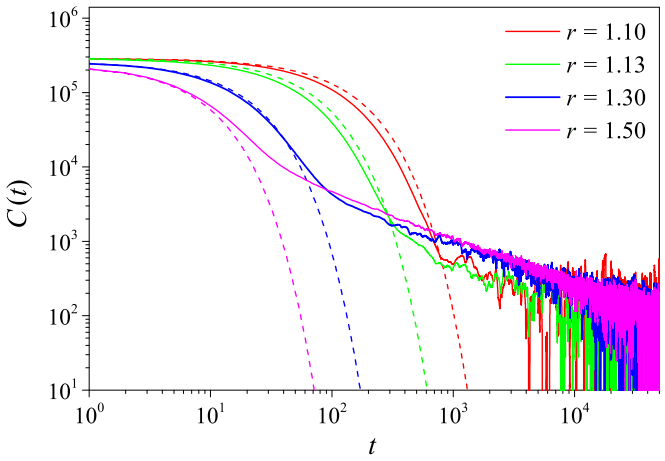

FIG. 1. The heat current autocorrelation function of the 1D diatomic gas model at various mass ratios. The solid lines are for simulation results, and the dashed lines of the same color are for the corresponding analytical predictions [Eq. (6)] based on our extended kinetic theory. In simulations, the system size is set to be $N = 50\,000$. Here and in all other figures, $k_B = 1$, $T = 1$, and $\mu_2 = 1$. From left to right, the pink, blue, green, and red lines are for $r = 1.50$, 1.30, 1.13, and 1.10, respectively.

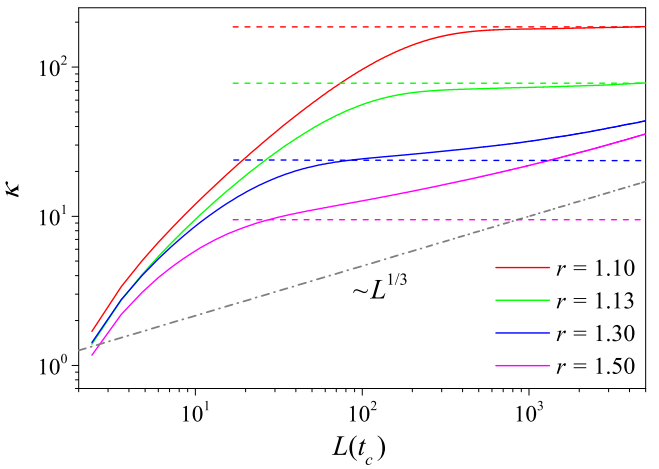

FIG. 2. The heat conductivity of the 1D diatomic gas model as a function of the system size at various mass ratios. The solid lines are for the results based on the Green-Kubo formula by integrating the heat current autocorrelation function numerically obtained. The horizontal dashed lines of the same color are for the corresponding result κ_k [Eq. (8)] due to the pure kinetic effect. From bottom to top, the pink, blue, green, and red lines are for $r = 1.50$, 1.30, 1.13, and 1.10, respectively.

has been worked out [9,10,26], which reads $C_H(t) = ct^{-(2/3)}$ in the thermodynamic limit. The parameter c is the amplitude of the power-law tail. Roughly, we can identify the time, denoted by t_1, that separates the kinetic and the hydrodynamic stages by

$$C(0)e^{-(t_1/\tau)} = ct_1^{-(2/3)}. \tag{9}$$

For $t < t_1$, the kinetic effect dominates. Because as $r \to 1$, both τ and t_1 increase [see Eqs. (7) and (13)], the kinetic region can last so long to allow the HCAF to decay for orders in the amplitude (see Fig. 1 for $r = 1.1$ as an example). On the other hand, for $t > t_1$, the hydrodynamic effect begins to take over, but its contribution to the heat conductivity will not be comparable before another time scale, denoted by t_2, that can be estimated by

$$\kappa_H = c\int_{t_1}^{t_2} t^{2/3}dt. \tag{10}$$

Namely, for $t > t_2$, we have $\kappa_H > \kappa_k$. The time scales t_1 and t_2 thus suggest two characteristic system sizes $L_1 = c_s t_1$ and $L_2 = c_s t_2$: For $L_1 < L < L_2$ we can expect that the heat conductivity is, in effect, independent of the system size. This is consistent with the previous numerical study [16] (see also Fig. 2 for $r = 1.1$ as an example).

Our method can also be adopted to study other 1D hard-core gas models. An immediate application is to the model with periodically repeating unit of one heavy particle of mass μ_1 and $Z-1$ light particles of mass μ_2. In this model, when two light particles collide, they simply exchange their velocities. Hence the dominant energy is transferred along the $Z-1$ light particles ballistically without any decay until the collision with a heavy particle occurs. As a result, the time t_F should be $Z-1$ times of that in the alternative diatomic gas, i.e., $t_F = \frac{(Z-1)a}{c_s}$. Hence Eqs. (6) and (7) do not change except that the value of t_F in (7) should be replaced.

Our method can be applied to models with random masses as well. Let us first consider the random diatomic gas model where a particle has a probability of $1/2$ to adjoin the same type of particles. The isotactic clusters formed have an average length of $\langle b\rangle = \sum_{i=0}^{+\infty} \frac{1}{2}^i a = 2a$, which implies that on average $t_F = \frac{2a}{c_s}$. So again we only need replace the value of t_F in Eq. (7). For the more general model where all the particles have random but close masses, on average after a collision the HCAF is

$$\langle J(t_F)J(0)\rangle = 8\left\langle \frac{m_i^2 m_{i+1}}{(m_i + m_{i+1})^3}\right\rangle C(0), \tag{11}$$

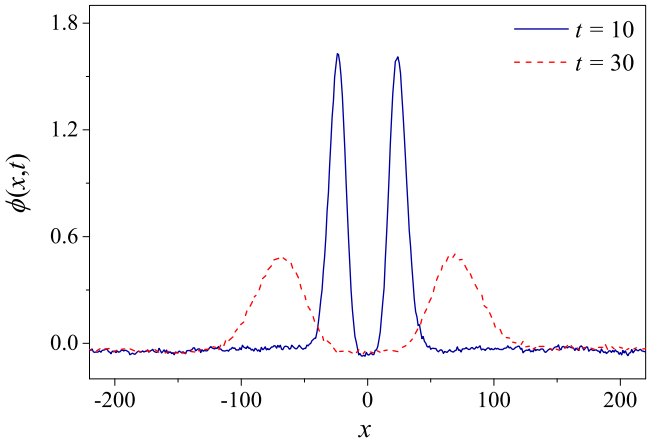

FIG. 3. The numerical simulation results of the spatiotemporal correlation functions of heat current density fluctuations of the 1D diatomic model with $r = 1.3$ at $t = 10$ (the blue solid line) and $t = 30$ (the red dashed line), respectively. By tracing the sound mode peaks the sound speed is measured numerically.

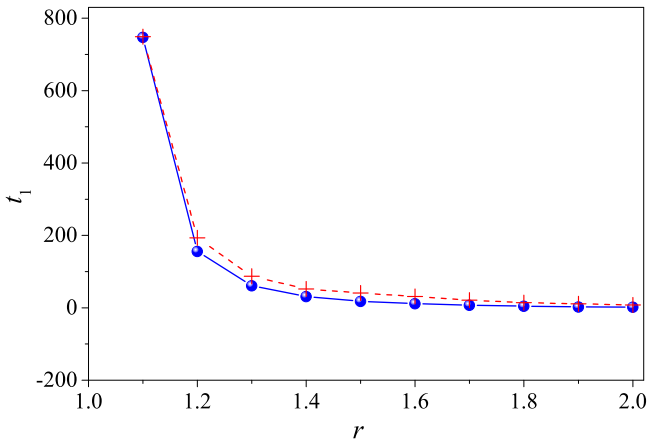

FIG. 4. Comparison of the time scale t_1 in the 1D diatomic gas model that separates the kinetic and hydrodynamic processes obtained by Eq. (9) analytically (the red crisscrosses) and by simulations (the blue bullets).

where $\langle \frac{m_i^2 m_{i+1}}{(m_i+m_{i+1})^3} \rangle$ is determined by the mass distribution. Suppose after time t the dominant carrier experiences P collisions, i.e., $t = Pt_F$, we have that the HCAF in the transient kinetic process also follows Eqs. (6) and (7) with

$$\tau = -t_F \left[\ln \left(\frac{m_i^2 m_{i+1}}{(m_i + m_{i+1})^3} \right) \right]^{-1}. \tag{12}$$

Now we put our analytical results into numerical check with the 1D diatomic gas model. As how to calculate analytically the sound speed of this model is still an open problem, we evaluate the sound speed by the aid of numerical simulations as well [27–29]. (Note that recently the sound speed for nonlinear 1D lattices with analytical interactions has been derived analytically [9], but, however, it does not apply to 1D fluid models.) In doing so, we measure the sound speed by tracing the motion of the sound mode peaks in the spatiotemporal correlation function of the heat current density fluctuations [29] (see Fig. 3). For $1.1 \leqslant r \leqslant 1.5$, we find that $c_s \approx 2.3$. For the HCAF, in our simulations, a system consisting of 50 000 particles with a periodic boundary condition is considered. The numerical results and the analytical results are compared in Fig. 1 for various mass ratios. We can see that the predicted HCAF based on the kinetic effect agrees with the simulation result very well in the transient time region $t < t_1$. In Fig. 2 we plot the corresponding thermal conductivity calculated by the Green-Kubo formula as a function of the system size where, for a given system size L, κ is measured by integrating $C(t)$ up to the truncated time $t_c = L/c_s$. It shows that the kinetic approach does allow us to predict the system-size-independent range of κ, which increases as $r \to 1$. For larger r this range disappears, although a crossover can be identified. The prediction fails for larger r since the hydrodynamic effect begins to play a significant role before the HCAF decays to a sufficiently small value. For example, for $r = 1.3$, the hydrodynamic contribution becomes dominant rapidly, and the power-law divergence of $\kappa \sim L^{1/3}$ can be recognized for $t > 10^3$ (see Fig. 2).

Next, we check the time scale t_1. To evaluate it by Eq. (9), in principle, we need to know the value of the parameter c. However, this parameter has not been solved yet by the hydrodynamic approach. (Note that the analytical approach developed by Mendl and Spohn [9] applies only to 1D lattices with analytical interactions.) Fortunately, we notice that t_1 does not depend on c sensitively. In fact, Eq. (9) can be rewritten as $\frac{t_1}{\tau} + \ln\left(\frac{c}{C(0)}\right) = \frac{2}{3}\ln(t_1)$. As for $r \to 1$, t_1 is large, whereas the term $\ln\left(\frac{c}{C(0)}\right)$ is negligible since $\frac{c}{C(0)} \sim 10^{-1}$ [26], we therefore can solve the following equation:

$$\frac{t_1}{\ln(t_1)} = \frac{2}{3}\tau \tag{13}$$

to estimate t_1. The result is shown in Fig. 4. One can see that it agrees very well with that obtained by simulations. (In simulations, t_1 is identified to be the convex-concave transition point of the HCAF.) From Fig. 4, it is seen that, for $r > 1.5$, t_1 drops to the order of 1, suggesting that the hydrodynamic region covers almost the entire time region. This is also consistent with previous numerical studies that claim the abnormal heat conduction with $r > 1.5$.

Finally, we present the results for other variant 1D hard-core gas models. In Figs. 5(a)–5(c), we compare the analytically predicted and the simulated HCAF for, respectively, the periodic model with repeating units of $\mu_1 - \mu_2 - \mu_2$, the random diatom model with binary isotactic clusters of μ_1 and μ_2, and

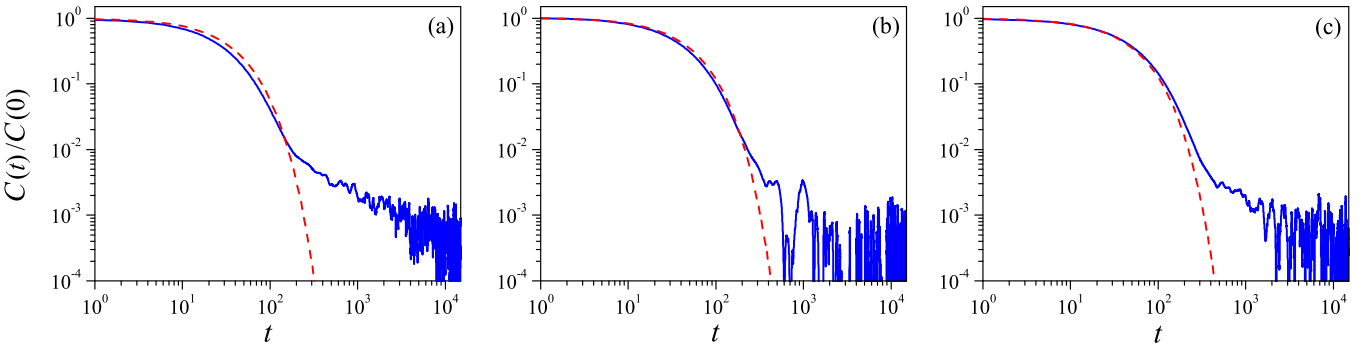

FIG. 5. The heat current autocorrelation function for three variant 1D gas models. (a) Periodic diatom model with repeating $\mu_1 - \mu_2 - \mu_2$ units. (b) Random diatomic gas model. In (a) and (b), $\mu_1 = 1.2$ and $\mu_2 = 1$. (c) Random gas model with the particle masses uniformly distributed between 1 and 1.4. In all the panels, the red dashed lines are for the theoretical prediction given by Eq. (6), and the blue solid lines are for the simulation result.

the random mass model with uniformly distributed masses $m_i \in (1, 1.4)$. In all three cases, the analytical results fit the simulation results very well in the kinetic region $t < t_1$.

To summarize, by introducing and tracing the tagged energy, we extend the kinetic approach to characterize the HCAF in the time region where the kinetic effect dominates. The system-size-independent heat conductivity observed in previous studies, including its value and the system-size range, is predicted quantitatively. Our Rapid Communication indicates that a full description of the HCAF should incorporate both the kinetic and the hydrodynamic effects. Our method may be applicable to other momentum conserving systems.

This work was partially supported by the Natural Science Foundation of China under Grants No. 11275179 and No. 11535011.

[1] M. Y. Han, J. C. Brant, and P. Kim, Electron Transport in Disordered Graphene Nanoribbons, Phys. Rev. Lett. **104**, 056801 (2010).

[2] A. M. Marconnet, M. A. Panzer, and K. E. Goodson, Thermal conduction phenomena in carbon nanotubes and related nanostructured materials, Rev. Mod. Phys. **85**, 1295 (2013).

[3] S. Lepri, R. Livi, and A. Politi, Thermal conduction in classical low-dimensional lattices, Phys. Rep. **377**, 1 (2003).

[4] A. Dhar, Heat transport in low-dimensional systems, Adv. Phys. **57**, 457 (2008).

[5] N. Li, J. Ren, L. Wang, G. Zhang, P. Hänggi, and B. Li, Colloquium: Phononics: Manipulating heat flow with electronic analogs and beyond, Rev. Mod. Phys. **84**, 1045 (2012).

[6] F. Bonetto, J. L. Lebowitz, and L. Rey-Bellet, *Mathematical Physics* (World Scientific, Singapore, 2000), p. 128.

[7] J. Wang and G. Casati, One-Dimensional Self-Organization and Nonequilibrium Phase Transition in a Hamiltonian System, Phys. Rev. Lett. **118**, 040601 (2017).

[8] P. I. Hurtado and P. L. Garrido, A violation of universality in anomalous Fourier's law, Sci. Rep. **6**, 38823 (2016).

[9] C. B. Mendl and H. Spohn, Dynamic Correlators of Fermi-Pasta-Ulam Chains and Nonlinear Fluctuating Hydrodynamics, Phys. Rev. Lett. **111**, 230601 (2013).

[10] H. van Beijeren, Exact Results for Anomalous Transport in One-Dimensional Hamiltonian Systems, Phys. Rev. Lett. **108**, 180601 (2012).

[11] S. Chen, Y. Zhang, J. Wang, and H. Zhao, Key role of asymmetric interactions in low-dimensional heat transport, J. Stat. Mech.: Theory Exp. (2016) 033205.

[12] S. Chen, Y. Zhang, J. Wang, and H. Zhao, Breakdown of the power-law decay prediction of the heat current correlation in one-dimensional momentum conserving lattices, arXiv:1204.5933.

[13] Y. Zhong, Y. Zhang, J. Wang, and H. Zhao, Normal thermal conduction in lattice models with asymmetric harmonic interparticle interactions, Chin. Phys. B **22**, 70505 (2013).

[14] A. V. Savin and Y. A. Kosevich, Thermal conductivity of molecular chains with asymmetric potentials of pair interactions, Phys. Rev. E **89**, 032102 (2014).

[15] S. Chen, Y. Zhang, J. Wang, and H. Zhao, Finite-size effects on current correlation functions, Phys. Rev. E **89**, 022111 (2014).

[16] S. Chen, J. Wang, G. Casati, and G. Benenti, Nonintegrability and the Fourier heat conduction law, Phys. Rev. E **90**, 032134 (2014).

[17] X. Xu, L. F. C. Pereira, Y. Wang, J. Wu, K. Zhang, X. Zhao, S. Bae, C. T. Bui, R. Xie, and J. T. L. Thong *et al.*, Length-dependent thermal conductivity in suspended single-layer graphene, Nat. Commun. **5**, 3689 (2014).

[18] M. H. Bae, Z. Li, Z. Aksamija, P. N. Martin, F. Xiong, Z. Y. Ong, I. Knezevic, and E. Pop, Ballistic to diffusive crossover of heat flow in graphene ribbons, Nat. Commun. **4**, 1734 (2013).

[19] G. Casati, Energy transport and the Fourier heat law in classical systems, Found. Phys. **16**, 51 (1986).

[20] P. L. Garrido, P. I. Hurtado, and B. Nadrowski, Simple One-Dimensional Model of Heat Conduction Which Obeys Fourier's Law, Phys. Rev. Lett. **86**, 5486 (2001).

[21] A. Dhar, Comment on "Simple One-Dimensional Model of Heat Conduction Which Obeys Fourier's Law", Phys. Rev. Lett. **88**, 249401 (2002).

[22] H. Li, Y. Wang, and H. Zhao, Comment on "Simple One-Dimensional Model of Heat Conduction Which Obeys Fourier's Law", Phys. Rev. Lett. **89**, 079401 (2002).

[23] P. Grassberger, W. Nadler, and L. Yang, Heat Conduction and Entropy Production in a One-Dimensional Hard-Particle Gas, Phys. Rev. Lett. **89**, 180601 (2002).

[24] J.-P. Hansen and I. R. McDonald, *Theory of Simple Liquids*, 3rd ed. (Academic, London, 2006).

[25] C. B. Mendl and H. Spohn, Equilibrium time-correlation functions for one-dimensional hard-point systems, Phys. Rev. E **90**, 012147 (2014).

[26] H. Spohn, Nonlinear fluctuating hydrodynamics for anharmonic chains, J. Stat. Phys. **154**, 1191 (2014).

[27] S. G. Das, A. Dhar, K. Saito, C. B. Mendl, and H. Spohn, Numerical test of hydrodynamic fluctuation theory in the Fermi-Pasta-Ulam chain, Phys. Rev. E **90**, 012124 (2014).

[28] L. Delfini, S. Denisov, S. Lepri, R. Livi, P. K. Mohanty, and A. Politi, Energy diffusion in hard-point systems, Eur. Phys. J.: Spec. Top. **146**, 21 (2007).

[29] H. Zhao, Identifying Diffusion Processes in One-Dimensional Lattices in Thermal Equilibrium, Phys. Rev. Lett. **96**, 140602 (2006).